# Structural and thermodynamic analyses reveal critical features of glycopeptide recognition by the human PILRα immune cell receptor

Received for publication, May 31, 2017, and in revised form, October 11, 2017 Published, Papers in Press, October 18, 2017, DOI 10.1074/jbc.M117.799239

Atsushi Furukawa[‡], Kosuke Kakita[§], Tomoki Yamada[¶], Mikihiro Ishizuka[‡], Jiro Sakamoto[‡], Nanao Hatori[§], Naoyoshi Maeda[¶], Fumina Ohsaka[¶], Takashi Saitoh[¶1], Takao Nomura[¶], Kimiko Kuroki[‡], Hisanori Nambu[§2], Hisashi Arase[‖**3], Shigeki Matsunaga[§], Masahiro Anada[§4], Toyoyuki Ose[‡], Shunichi Hashimoto[§], and Katsumi Maenaka[‡¶3,5]

*From the Laboratories of [‡]Biomolecular Science and [§]Synthetic and Industrial Chemistry, Faculty of Pharmaceutical Sciences and [¶]Center for Research and Education on Drug Discovery, Hokkaido University, Sapporo 060-0812, Japan and [‖]World Premier International Immunology Frontier Research Center and **Department of Immunochemistry, Research Institute for Microbial Diseases, Osaka University, Suita, Osaka 565-0871, Japan*

Edited by Peter Cresswell

**Before entering host cells, herpes simplex virus-1 uses its envelope glycoprotein B to bind paired immunoglobulin-like type 2 receptor α (PILRα) on immune cells. PILRα belongs to the Siglec (sialic acid (SA)-binding immunoglobulin-like lectin)-like family, members of which bind SA. PILRα is the only Siglec member to recognize not only the sialylated *O*-linked sugar T antigen (sTn) but also its attached peptide region. We previously determined the crystal structure of PILRα complexed with the sTn-linked glycopeptide of glycoprotein B, revealing the simultaneous recognition of sTn and peptide by the receptor. However, the contribution of each glycopeptide component to PILRα binding was largely unclear. Here, we chemically synthesized glycopeptide derivatives and determined the thermodynamic parameters of their interaction with PILRα. We show that glycopeptides with different sugar units linking SA and peptides (*i.e.* "GlcNAc-type" and "deoxy-GlcNAc-type" glycopeptides) have lower affinity and more enthalpy-driven binding than the wild type (*i.e.* GalNAc-type glycopeptide). The crystal structures of PILRα complexed with these glycopeptides highlighted the importance of stereochemical positioning of the O4 atom of the sugar moiety. These results provide insights both for understanding the unique *O*-glycosylated peptide recognition by the PILRα and for the rational design of herpes simplex virus-1 entry inhibitors.**

Paired immunoglobulin-like type 2 receptors (PILRs)[6] are surface proteins that are mainly expressed by immune cells, such as macrophages, dendritic cells, and granulocytes (1). PILRs form an archetypal paired receptor family, whose members typically include receptors with similar ectodomains but either inhibitory or stimulatory cytosolic signaling motifs. The inhibitory receptors such as PILRα incorporate an immunoreceptor tyrosine-based inhibition motif in the intracellular domain. By contrast, the activating receptors, such as PILRβ, incorporate a positively charged amino acid in the transmembrane region that associates with the activating adaptor subunit, DAP12 (2, 3). The endogenous ligands for PILRs include murine CD99 (4), PILR-associating neural protein (5), neuronal differentiation and proliferation factor-1, and collectin-12 (6). PILRα has a higher affinity for these ligands than PILRβ. Although the physiological effects of PILR binding to ligands remain largely unclear, *Pilrα*$^{-/-}$ mouse studies have shown increased neutrophil recruitment to inflammatory sites and increased susceptibility of the mice to endotoxin shock. Neutrophil recruitment in inflammatory responses is regulated by PILRα via modulation of integrin activation (7). PILRα is also the receptor for herpes simplex virus-1 (HSV-1), binding to its glycoprotein B (8). PILRs are sugar (sialic acid (SA))-binding

This work was supported in part by "Program for Advancing Strategic International Networks to Accelerate the Circulation of Talented Researchers" Grant S2701 (to K. M.); the Platform Project for Supporting in Drug Discovery and Life Science Research (Platform for Drug Discovery, Informatics, and Structural Life Science) from the Ministry of Education, Culture, Sports, Science and Technology (MEXT) and Japan Agency for Medical Research and Development (AMED); the Platform Project for Supporting Drug Discovery and Life Science Research funded by Japan AMED and Hokkaido University; and the Global Facility Center and Pharma Science Open Unit funded by MEXT under "Support Program for Implementation of New Equipment Sharing System." The authors declare that they have no conflicts of interest with the contents of this article.

This article contains supplemental Figs. S1–S5 and Table S1.

*The atomic coordinates and structure factors (codes 5XOF and 5XO2) have been deposited in the Protein Data Bank (http://wwpdb.org/).*

[1] Present address: Hokkaido Pharmaceutical University School of Pharmacy, Sapporo, Hokkaido 006-8590, Japan.

[2] Present address: Graduate School of Medicine and Pharmaceutical Sciences, University of Toyama, Sugitani, Toyama 930-0194, Japan.

[3] Supported by the Japan Society for the Promotion of Science Research and Core Research for Evolutional Science and Technology, Japan Science and Technology Corporation.

[4] Present address: Faculty of Pharmacy, Musashino University, Nishitokyo, Tokyo 202-8585, Japan.

[5] To whom correspondence should be addressed: Laboratory of Biomolecular Science, Faculty of Pharmaceutical Sciences, Hokkaido University, Kita-12, Nishi-6, Kita-ku, Sapporo 060-0812, Japan. Tel.: 81-11-706-3970; Fax: 81-11-706-4986; E-mail: maenaka@pharm.hokudai.ac.jp.

[6] The abbreviations used are: PILR, paired immunoglobulin-like type 2 receptor; HSV-1, herpes simplex virus-1; SA, sialic acid; ITC, isothermal titration calorimetry; Siglec, sialic acid-binding immunoglobulin-like lectin; r.m.s.d., root mean square deviation; sTn, sugar T antigen; Neu5Ac, *N*-acetylneuraminic acid; CLEC-2, C-type lectin-like receptor-2; Fmoc, *N*-(9-fluorenyl)methoxycarbonyl.

proteins and have part of a Siglec (sialic acid-binding immunoglobulin-like lectin)-like protein motif. It has been proposed that PILRα recognition of both endogenous and viral proteins is dependent on binding to both *O*-linked sugar T antigen (sTn) and peptide (9). The sTn antigen is produced by incomplete sugar modification, resulting in Neu5Ac(α2–6)GalNAc and GalNAc linked to threonine residues. Other reports have shown that the sTn antigen is not usually expressed on healthy cell surfaces but is often found on cancer cells (10). It is thus important to elucidate the detailed binding mechanisms between PILRα and sTn peptide to better understand its role in immune cell responses to tumors and infection.

Recently, we reported the crystal structure of PILRα complexed with the GalNAc-type glycopeptide (9). This result indicated that PILRα simultaneously recognized both saccharide, especially the terminal SA, and peptide components. However, the precise contribution of each glycopeptide component to the strength and specificity of PILRα binding remains unclear. In this current study, we first determined the thermodynamic parameters necessary for the interaction between PILRα and GalNAc-type glycopeptide to better understand the mechanism for PILRα and glycopeptide interaction. This revealed that both the enthalpy and entropy contributed to PILRα binding to glycopeptides. Next, we synthesized glyco (and glyco analog)-peptide compound derivatives in which the sugar link between SA and *O*-linked Thr is GalNAc (wild type), GlcNAc, or deoxy-GlcNAc (with the hydroxyl group at position 4 replaced with hydrogen) and evaluated the affinity of their interactions with PILRα. The altered glycopeptides (hereafter GlcNAc-type glycopeptide and deoxy-GlcNAc-type glycopeptide) exhibited lower binding affinity than the wild-type GalNAc-type glycopeptide. To understand the detailed molecular mechanism of this reduction in binding affinity, we successfully determined the complex structures of PILRα with GlcNAc-type or deoxy-type glycopeptides by X-ray crystallography. Our results demonstrate the importance of each component of the glycopeptide for optimal stereochemical positioning of the sugar atoms that bind to PILRα. This study also further clarifies the molecular basis for the contribution of glycan and peptide binding to PILRα and provides novel insights for the rational design and development of HSV-1 entry inhibitors and immune checkpoint regulators.

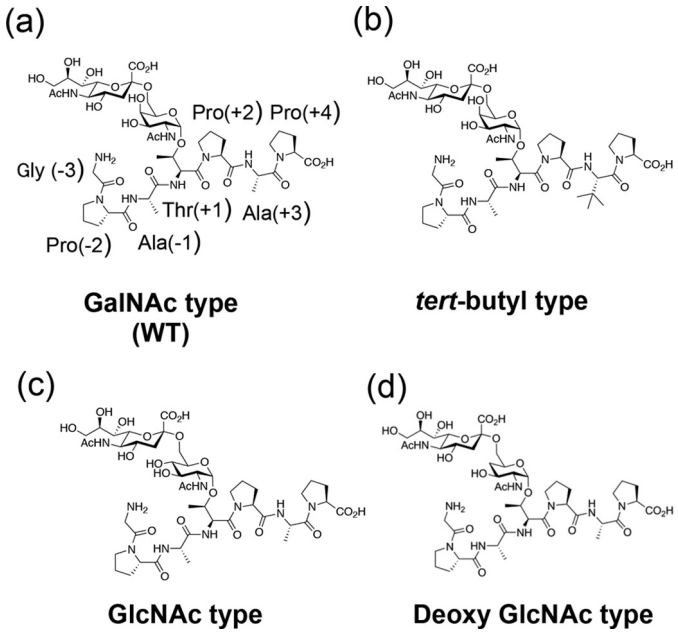


**Figure 1. The synthetic and wild-type glycopeptides used in this study.** *a*, GalNAc type (wild type); *b*, *tert*-butyl type; *c*, GlcNAc type; *d*, deoxy-GlcNAc type.

## Results

### *Thermodynamic properties of PILRα binding to HSV-1 gB GalNAc-type glycopeptide*

Recently, we reported the crystal structure of PILRα complexed with a 7-mer GalNAc-type glycopeptide derived from the N-terminal region of HSV-1 gB ($Gly^{50}$–$Pro^{56}$) (Fig. 1*a*). The complex structure indicated that PILRα recognized terminal SA through a well-ordered network of hydrogen bonds and electrostatic interactions. Furthermore, a substantial conformation change in a region that contains hydrophobic amino acid residues, especially $Phe^{76}$ and $His^{77}$ in the CC′ loop, was observed upon binding of proline and GalNAc of the glycopeptide to the receptor (9). To evaluate the physicochemical parameters of this interaction, we performed an isothermal titration calorimetry (ITC) experiment. The GalNAc-type glycopeptide (1 mM) was titrated into a 50 μM PILRα solution. The dissociation constant ($K_d$) of the interaction is 6.7 ± 1.6 μM, determined by two independent experiments and calculated to fit well with a 1:1 binding model (Fig. 2*a* and Table 1). This $K_d$ value was similar to the affinity determined using the flexible N-terminal region of gB (amino acid residues 30–108) in surface plasmon resonance analysis (~2.8 μM) and competition assays (a few μM) (9). We also titrated the SA, sTn-threonine, and GPATPAP peptide constituents of the GalNAc-type glycopeptide with PILRα, but none of them bound with detectable affinity (Fig. 3). These results supported the previous notion that simultaneous recognition of both sugar and peptide is necessary for binding to PILRα. This interaction is mainly enthalpy-driven with preferable entropy ($\Delta H = -5.8$ kcal/mol and $-T\Delta S = -1.2$ kcal/mol at 25 °C). The observation of an enthalpy–entropy-driven reaction is consistent with the fact that PILRα binds to the SA region of the GalNAc-type glycopeptide through hydrogen bonds and ionic interactions and to its peptide part through van der Waals interaction.

### *Thermodynamic property of the interactions of PILRα with tert-butyl-type glycopeptide*

Our previous structural analysis indicated that Pro (+2) of the GalNAc-type glycopeptide, which is adjacent to Thr (+1) attached to *O*-glycan, interacts with $Phe^{76}$ and $His^{77}$ of PILRα. Further C-terminal amino acid residues, adjacent to the *O*-glycosylated threonine, form a turn structure that widely engages with the loop of PILRα. Increases in peptide chain flexibility can reduce the binding affinity of some protein-ligand interactions (11, 12). We thus sought to determine whether Ala (+3), which has a small side chain and presumably enhances flexibility,

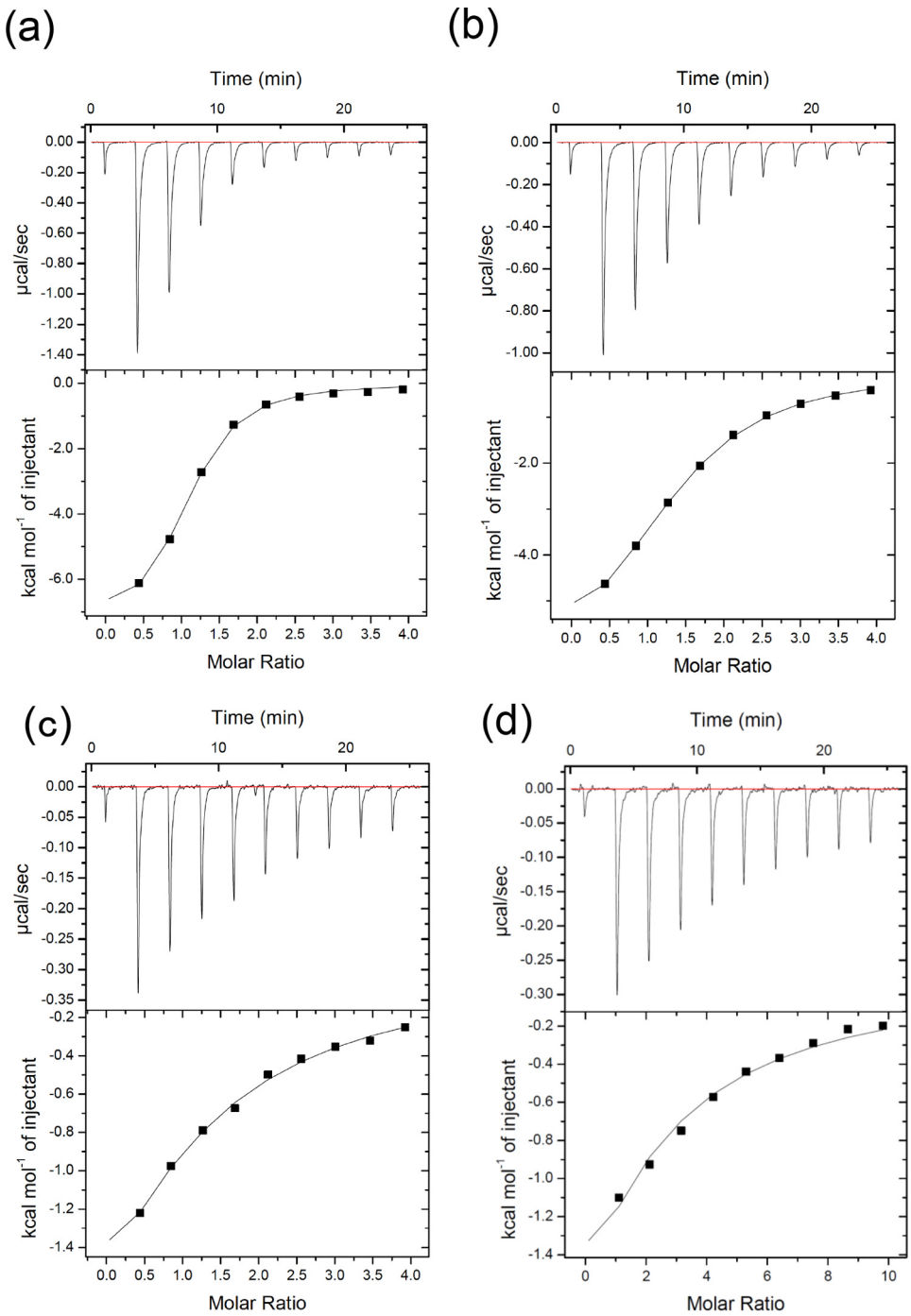


**Figure 2. ITC measurements for PILRα binding to wild-type and synthetic glycopeptides.** *Upper panels* show the representative titration thermograms, and *lower panels* show the data integration with fitted curves (1:1 binding model) of GalNAc-type (*a*), *tert*-butyl-type (*b*), GlcNAc-type (*c*), and deoxy-GlcNAc-type (*d*) glycopeptides with PILRα. The fitting error estimates were calculated using a 1:1 binding model and are as follows: *a*, $K_d = 5.1 \pm 0.1$ μM, $\Delta H = -7.2 \pm 0.0$ kcal/mol; *b*, $K_d = 21.9 \pm 0.9$ μM, $\Delta H = -6.8 \pm 0.1$ kcal/mol; *c*, $K_d = 97.1 \pm 5.4$ μM, $\Delta H = -4.0 \pm 0.1$ kcal/mol; *d*, $K_d = 120.6 \pm 11.4$ μM, $\Delta H = -9.5 \pm 0.5$ kcal/mol.

could be modified to reduce glycopeptide flexibility. Thus, a *tert*-butyl modification was introduced to the side chain of Ala (+3) (Fig. 1*b*). The ITC experiment using the bulky *tert*-butyl-modified Ala (+3) unnatural glycopeptide (*tert*-butyl-type glycopeptide) determined a $K_d$ of 18 μM for the interaction with PILRα (Fig. 2*b* and Table 1). This indicated that the *tert*-butyl group modification of Ala (+3) did not result in the expected increase in binding but rather slightly decreased the affinity of glycopeptide for PILRα. Thermodynamic parameters for the interaction indicated that it was enthalpy-driven with a small preferable entropy component ($\Delta H = -6.0 \pm 0.8$ kcal/mol and $-T\Delta S = -0.7 \pm 0.7$ kcal/mol at 25 °C) (Fig. 2*b* and Table 1). These parameters were similar to those derived for interactions of PILRα with the wild-type peptide (Table 1). This result suggested that the addition of bulky side chains to the peptide region, which probably does not form a direct contact with PILRα, is not sufficient to change the binding characteristics.

**Table 1**
**Thermodynamic parameters of PILRα binding**
The values are means ± ranges derived from two independent experiments calculated using a 1:1 binding model. Representative binding data for one of the two experiments is shown in Fig. 2.

| | Ligand | | | |
|---|---|---|---|---|
| | GalNAc type | *tert*-Butyl type | GlcNAc type | Deoxy-GlcNAc type |
| $\Delta G$ (kcal/mol) | −7.1 ± 0.2 | −6.7 ± 0.0 | −5.5 ± 0.0 | −5.5 ± 0.2 |
| $-T\Delta S$ (kcal/mol) | −1.2 ± 1.2 | −0.7 ± 0.7 | −1.4 ± 0.1 | 2.2 ± 1.9 |
| $\Delta H$ (kcal/mol) | −5.8 ± 1.3 | −6.0 ± 0.8 | −4.1 ± 0.1 | −7.7 ± 1.8 |
| $N$ | 0.98 | 1.27 | | |
| $K_A$ ($M^{-1}$) | $1.6 \times 10^5$ | $6.1 \times 10^4$ | $10 \times 10^3$ | $12 \times 10^3$ |
| $K_d$ (μM) | 6.7 | 18 | 98 | 94 |

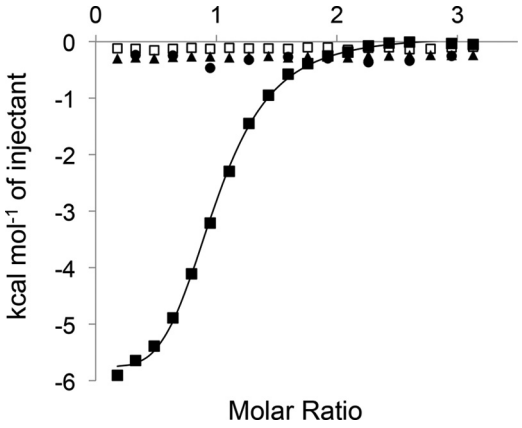


**Figure 3. ITC measurements for PILRα binding to isolated components of the GalNAc-type glycopeptide.** Titration isothermograms of PILRα with the different glycopeptide components are shown. ■, GalNAc-type glycopeptide; ▲, sTn-threonine; ●, GPATPAP; □, SA.

### *Effect of changing the GalNAc sugar moiety in the wild-type glycopeptide on the thermodynamic properties of binding interactions with PILRα*

Our previous published crystal structure of the PILRα–GalNAc-type glycopeptide indicated that GalNAc does not significantly contribute to PILRα binding to glycopeptides. Thus, this region could be a potential target site for modification to alter the affinity of glycopeptide. To verify the role of GalNAc, we synthesized two glycopeptides with the substitution of either GlcNAc-type glycopeptide (GlcNAc type) (Fig. 1*c*) or deoxy-GlcNAc-type glycopeptide (deoxy type) (Fig. 1*d*) with GalNAc. Neither of these synthetic glycopeptides occurs naturally. GlcNAc-type and deoxy-type glycopeptides have a different orientation (equatorial) and a loss of the hydroxyl group at position 4 (4-OH), respectively. We determined the dissociation constants and thermodynamic parameters of the interactions of these altered peptides by ITC. Both unexpectedly and notably, a great reduction of the affinity of GlcNAc-type glycopeptide for PILRα was observed (98 ± 1.0 μM) (Fig. 2*c* and Table 1). Thermodynamic parameters of the interaction showed an enthalpy-driven reaction with a small favorable entropy effect ($\Delta H = -4.1$ kcal/mol and $-T\Delta S = -1.4$ kcal/mol at 25 °C). Furthermore, we also found that the $K_d$ of the deoxy-type glycopeptide binding to PILRα (94 ± 26 μM) is weaker than that of the GalNAc-type (Fig. 2*d* and Table 1). Thermodynamic parameters for the interaction between PILRα and the deoxy-type glycopeptide showed a more unfavorable entropy effect ($\Delta H = -7.7$ kcal/mol and $-T\Delta S = 2.2$ kcal/mol at 25 °C) than the GalNAc-type peptide. Although the hydroxyl group at position 4 of GalNAc is not directly involved in the interaction with PILRα, it nevertheless contributes to the interaction with PILRα with favorable entropy.

### *Crystallographic analyses of PILRα–GlcNAc-type and –deoxy-type glycopeptide complexes*

To determine the molecular mechanism for the reduced affinity of GlcNAc-type and deoxy-type glycopeptides for PILRα, we performed X-ray crystallographic studies of the PILRα complexes with these two glycopeptides. Crystals of PILRα complexed with a 5-fold molar ratio excess of each GlcNAc-type glycopeptide were successfully obtained in 0.1 M Tris-HCl (pH 8.5) and 25% PEG6000. Crystals for the deoxy-GlcNAc-type complex were grown in 0.1 M MES monohydrate (pH 6.5) and 1.6 M magnesium sulfate heptahydrate. The diffraction data were collected at SPring-8 (Harima, Japan) with 1.96-Å resolution using the BL44XU beamlines for the GlcNAc-type complex and 2.2-Å resolution using the BL32XU beamlines for the deoxy-type complex. The crystallographic parameters are summarized in Table 2. Four complexes were observed in the asymmetric unit in the PILRα–GlcNAc-type glycopeptide complex that were essentially the same as the GalNAc type (root mean square deviation (r.m.s.d.) = 0.20–0.43 Å) (supplemental Fig. S1). Two chains were observed in the asymmetric unit in the deoxy-type complex; both bound glycopeptide without any significant changes (r.m.s.d. = 0.24 Å) (supplemental Fig. S2). In both complexes, the conformations of peptides between each chain were also hardly changed (PILRα complexed with GlcNAc-type or deoxy-GlcNAc-type glycopeptide is shown in supplemental Figs. S3 and S4, respectively). Thus, we use chain A in both complex structures as a representative chain hereafter.

### *Structural comparison of PILRα–GalNAc-type, –GlcNAc-type, and –deoxy-GlcNAc-type glycopeptide complexes*

The crystal structures of PILRα complexes with the GlcNAc- and deoxy-GlcNAc-type glycopeptides and GalNAc type are shown in Fig. 4, *a–c*. The electron density maps clearly show that the synthetic GlcNAc-type and deoxy-GlcNAc-type glycopeptides exhibit the equatorial orientation and loss of the hydroxyl group, respectively, as shown in Fig. 4, *d–f*. The superimposition of the complex structures showed that GlcNAc type (*light pink*) and deoxy-GlcNAc type (*yellow*) are essentially the same, but in contrast, the GalNAc-type complex structure (*green*) does not fit well with the others (Fig. 4*g*). Next, we closely examined the binding sites and compared the molecular/atomic distances for each interaction. The key residues of PILRα for binding to GalNAc type are $Tyr^{33}$, $Arg^{126}$, $Gln^{138}$, and $Gln^{140}$ for binding to the sialic acid moiety; $Phe^{76}$ for binding to the peptide moiety; and $His^{77}$ for binding to both GalNAc and peptide. The superimposed structure of the interface and distances of essential interactions for the three complex structures are summarized in Fig. 5, *a–d*, and supplemental Table S1. Almost all of interactions with sialic acid are conserved. The carbonate group of the sialic acid residue interacts directly with

**Table 2**
**Crystallographic parameters for the PILRα–GlcNAc and –deoxy-GlcNAc-type glycopeptide complexes**

| | GlcNAc-type glycopeptide–PILRα complex | Deoxy-GlcNAc-type glycopeptide–PILRα complex |
|---|---|---|
| **Data collection** | | |
| Space group | *P*21 | *C*2 |
| Cell dimensions | | |
| *a*, *b*, *c* (Å) | 54.66, 63.01, 78.6 | 81.28, 63.33, 55.07 |
| α, β, γ (°) | 90, 108.3, 90 | 90, 110.8, 90 |
| Resolution (Å)[a] | 50–1.96 (1.99–1.96) | 50–2.2 (2.24–2.2) |
| $R_{merge}$[a] | 0.105 (0.322) | 0.054 (0.169) |
| $I/\sigma(I)$[a] | 20.9 (5.5) | 25.0 (8.4) |
| Completeness (%) [a] | 99.4 (96.35) | 99.9 (99.7) |
| Redundancy[a] | 3.8 (3.8) | 3.8 (3.6) |
| Total no. of observations[a] | 137,800 | 51,035 |
| Unique reflections[a] | 36,271 (1,754) | 13,393 (668) |
| **Refinement** | | |
| No. of reflections (work/test) | 32,742/1,670 | 12,752/673 |
| Resolution (Å)[a] | 40.05–1.963 (2.033–1.963) | 40.14–2.201 (2.279–2.201) |
| $R_{work}$[a] | 0.2145 (0.2671) | 0.2163 (0.2352) |
| $R_{free}$[a] | 0.2692 (0.3341) | 0.2616 (0.3188) |
| No. of atoms | | |
| Protein | 4,116 | 2,058 |
| Ligand | 136 | 66 |
| Water | 258 | 49 |
| B factors | | |
| Protein | 18.86 | 33.16 |
| Ligand | 16.85 | 25.46 |
| Water | 24.47 | 34.10 |
| r.m.s.d. | | |
| Bond lengths (Å) | 0.009 | 0.008 |
| Bond angles (°) | 1.50 | 1.44 |
| Ramachandran plot statistics | | |
| Most favored (%) | 97.35 | 95.53 |
| Disallowed (%) | 0 | 0.41 |

[a] Statistics for the highest-resolution shell are shown in parentheses.

guanidine group of $Arg^{126}$ in all complexes (2.7 and 2.9 Å in PILRα–GalNAc type, 2.8 and 3.1 Å in PILRα–GlcNAc type, and 2.8 and 3.1 Å in PILRα–deoxy-GlcNAc type) (Fig. 5*c* and supplemental Table S1). The amide and carbonyl groups of the main chain of $Gln^{138}$ and $Gln^{140}$ interact with the hydroxyl group of the glycerol part and amide group of the *N*-acetyl group of SA, respectively, in all complexes. $Tyr^{33}$ also interacts with SA in a similar manner. These observations indicate that the interactions of PILRα with SA of the three different glycopeptides are almost unchanged. In contrast, the interactions of $Phe^{76}$ and $His^{77}$ with the different ligands are different between the different complexes. $Phe^{76}$ makes van der Waals contacts with the hydrophobic pyrrolidine rings of proline residues in the C-terminal part of the GalNAc-type sTn peptide (a distance of 3.4 Å; Fig. 5*a*, *white dotted line*). This distance increases to create weak contacts in the other complexes (3.8 Å in GlcNAc type and 4.1 Å in deoxy-GlcNAc type) (Fig. 5, *a* and *d*). Previous results also indicated that $His^{77}$ forms a hydrogen bond with the carboxyl group of Pro (+2) (Fig. 5*a*, *black dotted line*) and a van der Waals contact with GalNAc (Fig. 5*a*, *silver dotted line*) (9). Although these hydrogen bonds have similar distances in the three complexes (2.6 (GalNAc), 2.8 (GlcNAc), and 2.8 Å (deoxy-GlcNAc)), the distances between $His^{77}$ and the linker sugars are changed between the three complexes (Fig. 5, *b* and *d*). In the PILRα–GalNAc-type complex, the imidazole ring of $His^{77}$ forms a small contact distance with not only the 4-OH but also the whole hexose ring of the GalNAc sugar linker (supplemental Table S1). By contrast, the 4-OH hydroxyl group of GlcNAc does not face $His^{77}$ in the GlcNAc-type complex. There is no hydroxyl group on this part of the sugar linker of the deoxy-GlcNAc-type glycopeptide. These structural differences reduce both the hydrophobic $Phe^{76}$-proline and $His^{77}$-linker sugar interactions, which contributes to the loss of the entropy effect observed in the ITC measurements.

## Discussion

Our previous study showed that the affinity between PILRα and the N-terminal region (amino acids 30–108) of gB is 2.3 μM and that the glycopeptide part, GPAT(sTn)PAP (amino acids 50–56), of this region is essential and was successfully cocrystallized with PILRα (9). In this study, we consistently determined the dissociation constant of the PILRα binding of GalNAc-type peptide (wild type), GPAT(sTn)PAP, to be 6.7 μM by ITC. We also characterized the thermodynamic properties of PILRα binding to synthetic peptides. The wild-type GalNAc-type glycopeptide has entropy–enthalpy-driven binding to PILRα. While we solved the crystal structures of PILRα (Protein Data Bank code 3WUZ) and its complex with the glycopeptide (Protein Data Bank code 3WV0) (9), Lu *et al.* concurrently reported the crystal structures of unliganded PILRα (Protein Data Bank code 4NFB) and PILRβ (Protein Data Bank code 4NFC) (13). Comparison of these structures indicates that the CC′ loop of the PILRαs undergoes dramatic rearrangements upon glycopeptide binding. Interestingly, however, the CC′ loop of the unliganded PILRβ maintains a conformation similar to that of liganded PILRα (supplemental Fig. S5). As the sequence is highly conserved between PILRα and PILRβ in this CC′ loop-binding region, these data imply that the CC′ loops of PILRs intrinsically have large flexibility with the predominant conformations selected for upon glycopep-

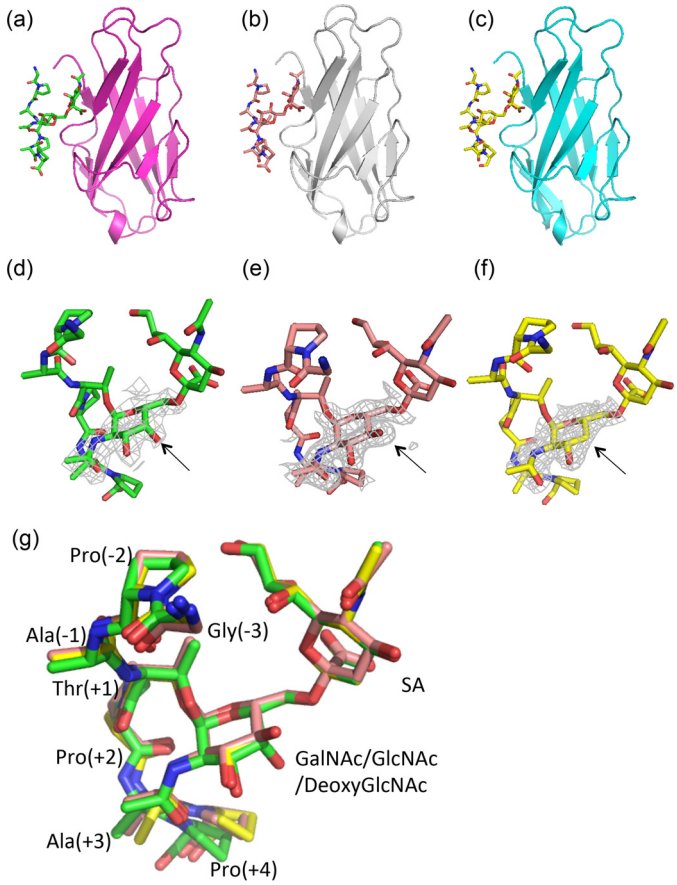


**Figure 4. Crystallographic analysis of PILRα complexed with GlcNAc-type and deoxy-GlcNAc-type glycopeptides.** *a–c*, the superimposed complex structures of GalNAc-type glycopeptide (*green*)–PILRα (*light purple*) (from Protein Data Bank code 3VW0) (9) (*a*), GlcNAc-type glycopeptide (*light pink*)–PILRα (*gray*) (*b*), and deoxy-GlcNAc-type glycopeptide (*yellow*)–PILRα (*light blue*) (*c*) are shown. *d–f*, the structures of GalNAc-type (*d*), GlcNAc-type (*e*), and deoxy-GlcNAc-type (*f*) glycopeptides with composite omit map ($2F_o - F_c$ map) on the linker sugar are shown. The electron density map is contoured at 1.0$\sigma$, and resolutions are 2.3, 2.0, and 2.2 Å, respectively. *Arrows* indicate the altered stereochemistry or loss of the sugar hydroxyl group. *g*, the structures of the glycopeptides superimposed at sialic acid in the complex with PILRα were extracted from the complex structures. The color of each glycopeptide is the same as in *d–f*.

tide binding. Indeed, this is consistent with our ITC experiments, which revealed no significant entropic loss upon glycopeptide complex formation.

Next, we introduced modifications of both peptide and sugar regions to determine their roles in binding and whether modification of linker residues could be developed for further rational inhibitor design. The *tert*-butyl modification of Ala (+3), aimed at reducing excessive flexibility in the peptide region, did not produce any significant changes in binding characteristics. It is possible that this modification may not reduce the flexibility sufficiently to affect binding and further modifications, such as introduction of a double bond in the peptide backbone, may further determine the contribution of peptide to binding. Conversely, the slight modification of a 4-OH group in the linker sugar GalNAc markedly reduced binding affinity, revealing the importance of the linker sugar for the formation of a well-ordered binding network with PILRα. Comparison of the crystal structures of the different complexes clearly reveals that the direction or absence of 4-OH in the linker sugars slightly alters the network of binding interactions. This impacts a wide area of the interface, causing the C-terminal peptide part far from the linker sugar to be more distant from the protein surface of the CC′ loop, resulting in less hydrophobic interactions between PILRα and either GlcNAc-type or deoxy-GlcNAc-type glycopeptides compared with the GalNAc-type glycopeptide. These changes in interactions contribute to the unfavorable entropic effect with the modified glycopeptides. This suggests that the sugar characteristics are finely tuned for the binding. Together these observations support that the global interaction network with both glycan and peptide parts of glycopeptides should be considered for designing better inhibitors for PILRα.

Proline residues at the adjacent C-terminal part of glycosylated threonine have been previously proposed to be important for receptor binding (9). In this study, we showed that sTn-threonine could not bind PILRα and verified the necessity of additional residues, including adjacent proline(s), for receptor interactions. The frequent appearance of a proline residue at an *O*-linked glycosylation site (14) may facilitate simultaneous recognition of sialic acid and proline(s), which would be beneficial for immune surveillance by PILRα. In contrast, the recent structures of sialic acid-containing glycopeptide recognition proteins, such as C-type lectin-like receptor-2 (CLEC-2), reveal a different binding mechanism (15). The complex structure of CLEC-2 with glycopeptide, derived from the ligand podoplanin, revealed the importance of terminal sialic acid and aspartic acid and glutamic acid at the N-terminal part of the attached peptide for receptor binding. Both the proline residue in the C-terminal region, adjacent to the glycosylated threonine, and the GalNAc of the glycopeptide are not involved in the interaction with CLEC-2. These results demonstrate that, although both PILRα and CLEC-2 can be categorized as sTn peptide-recognition proteins, they have different mechanisms for binding to ligands.

In summary, we synthesized various kinds of glycopeptides with modifications of either peptide or sugar moieties and determined both their binding affinities and their crystal structures with PILRα. Although PILRα exhibits essentially the same recognition of the different glycopeptides, slight modifications of the linker sugar cause significant changes in a wide area of the binding interface, resulting in a reduction of binding affinity. The findings of the present study provide insights into the mechanism of glycoprotein recognition by PILRα and contribute to the rational drug design of HSV-1 entry inhibitors.

## Materials and methods

### *Synthesis of glycopeptides*

The method for synthesizing the glycopeptides in Fig. 1 will be described in a separate publication[7] (16). In brief, sialyl Tn-glycopeptides were synthesized by solid-phase peptide synthesis based on the Fmoc strategy using protected sialyl Tn antigen building blocks. The requisite disaccharide-threonine building blocks were prepared from FmocThrOBn (where

[7] K. Kakita, N. Hanari, M. Anada, H. Nambu, A. Furukawa, J. Sakamoto, K. Kuroki, T. Saitoh, S. Matsunaga, K. Maenaka, and S. Hashimoto, manuscript in preparation.

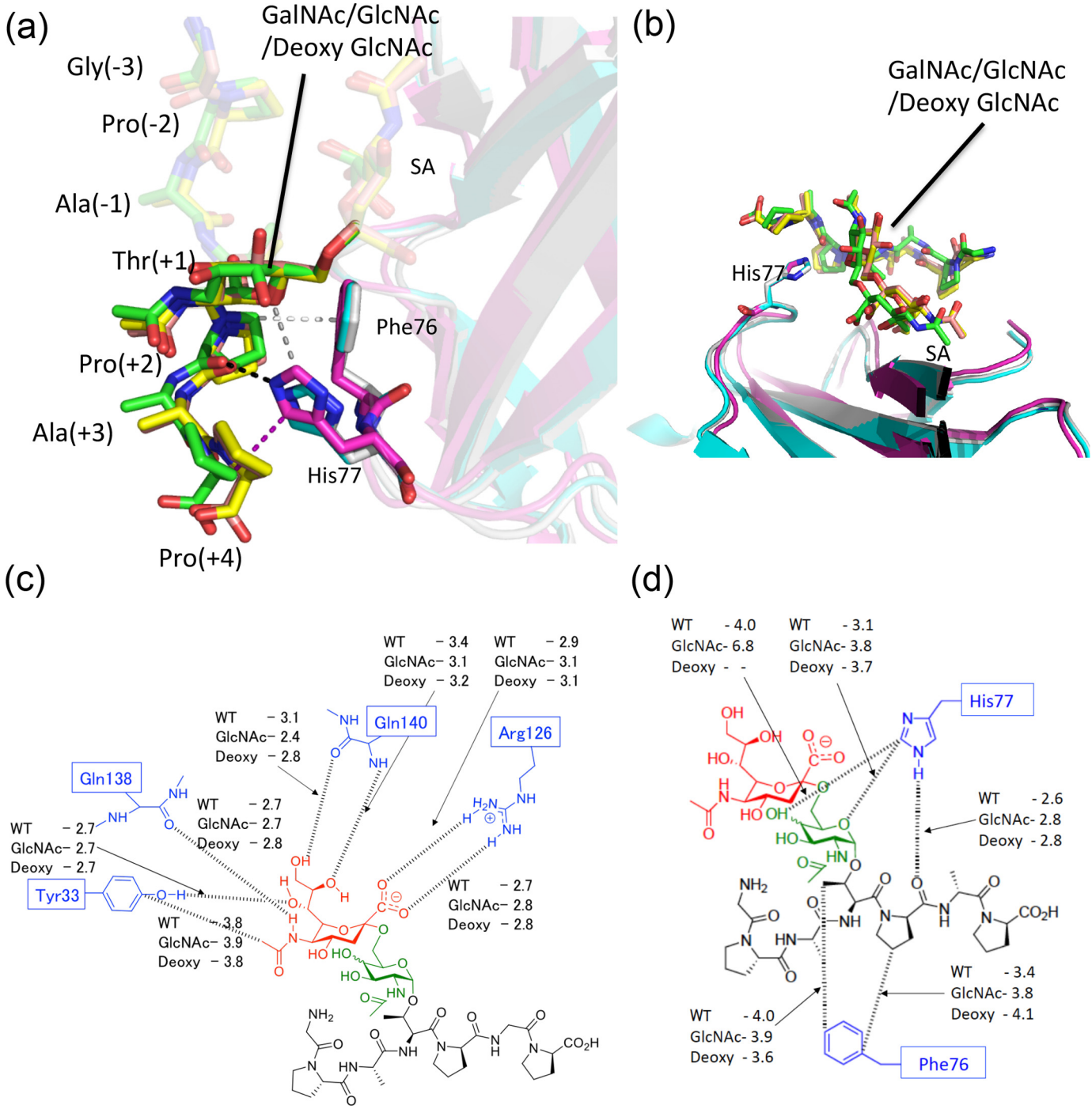


**Figure 5. Close-up view of the interfaces of PILRα with glycopeptides.** *a* and *b*, close-up view of the interactions between Phe[76] and His[77] from PILRα and the linker sugar and peptide part of the different glycopeptides are shown. The superimposed complex structures of PILRα (*light purple*)–GalNAc-type (*green*) (from Protein Data Bank code 3VW0), PILRα (*gray*)–GlcNAc-type (*light pink*), and PILRα (*light blue*)–deoxy-GlcNAc-type glycopeptide (*yellow*) are shown. Superimpositions of the three complexes showing amino acid residues that are involved in sialic acid binding (*a*) and the imidazole ring of His[77] (*b*) of PILRα are shown. *Dashed lines* represent interactions with PILRα–GalNAc-type glycopeptide. *c* and *d*, a schematic representation of the simultaneous recognition of glycopeptide (interactions around sialic acid are shown in *a*) and linker sugar and peptide (shown in *b*) region by PILRα. SA (*red*), GalNAc (*green*), the peptide region (*black*), and PILRα residues (*blue*) are shown. The distances of interactions in each complex are shown. The unit of distance represented is Å.

Bn is benzyl) via glycosylation with glycosyl diphenyl phosphates followed by triflic acid-promoted coupling with sialyl diethyl phosphite (16).[7]

### *Expression and purification of PILRα*

Expression and purification of PILRα were performed as reported previously (17). Briefly, the extracellular domain of PILRα (residues 32–150) was cloned into pGMT7 vector (17). The resulting plasmid was transformed into *Escherichia coli* Rosetta2 (DE3) (Millipore), and the PILRα protein was expressed as inclusion bodies. The inclusion bodies were washed, solubilized with guanidine buffer, and refolded using the standard dilution method (18). The refolded PILRα was purified by gel filtration chromatography followed by Resource

S column chromatography (GE Healthcare). Purified PILRα was preserved and maintained in buffer containing 20 mM succinate (pH 5.0) and 100 mM NaCl.

### *Isothermal titration calorimetry*

The thermodynamic parameters for the binding of PILRα and glycopeptides were determined by ITC (Macrocal iTC200, Malvern). The cell and syringe were filled with 50 μM PILRα and 1 mM ligands (GalNAc type and *tert*-butyl type) in HBS-P buffer (10 mM HEPES, 150 mM NaCl, and 0.05% (v/v) surfactant P20), respectively. Each experiment consisted of a single 2-μl injection of the different ligands into the PILRα solution. For studying the binding of lower-affinity glycopeptides GlcNAc-type glycopeptide (50 μM PILRα and 1 mM ligand) and deoxy-GlcNAc-type glycopeptide (20 μM PILRα and 1 mM ligand), each experiment consisted of a single 4-μl injection of ligands into the PILRα solution to overcome the low heat generated by weak interactions, adopting previously described methods (19, 20). Data analysis was performed with the software package Origin 5.0. The integrated heats generated in the experiments were fitted using a single-site binding model.

### *Crystallization of PILRα complexed with glycopeptide*

The crystallization of PILRα complexed with glycopeptides was performed following procedures similar to those described previously for the PILRα–gB sTn glycopeptide complex (9, 17). The sitting drop consisted of a mixture of 0.2 μl of PILRα complex solution (40 μM) including GlcNAc-type glycopeptide or deoxy-GlcNAc-type glycopeptide (200 μM) (20 mM succinate (pH 5.0) and 100 mM NaCl) and 0.2 μl of reservoir solution. The crystallization well included 90 μl of reservoir buffer at 293 K. Crystals of the PILRα–GlcNAc-type glycopeptide and –deoxy-GlcNAc-type glycopeptide complexes were obtained using PEGs Suite Number 45 buffer (0.1 M Tris-HCl (pH 8.5) and 25% (w/v) PEG6000) and Crystal Screen 2 Number 20 buffer (0.1 M MES monohydrate (pH 6.5) and 1.6 M magnesium sulfate heptahydrate) as reservoir solutions, respectively.

### *Data collection and structure determination*

A diffraction data set was collected in SPring-8 (Harima, Japan) at 100 K on beamline BL44XU for the PILRα–GlcNAc-type glycopeptide complex and BL32XU for the PILRα–deoxy-GlcNAc-type glycopeptide complex. The structure was phased by molecular replacement using Molrep in the CCP4 package (21) using the GalNAc-type glycopeptide-binding PILRα (Protein Data Bank code 3WV0) structure as a search probe. The crystals of PILRα–GlcNAc-type glycopeptide belonged to the space group $P2_1$ with unit cell dimensions of $a = 54.66$ Å, $b = 63.01$ Å, $c = 78.60$ Å, $\alpha = \gamma = 90°$, and $\beta = 108.34°$ and contained four molecules per asymmetric unit. The crystals of PILRα–deoxy-GlcNAc-type glycopeptide belonged to the space group $C2$ with unit cell dimensions of $a = 81.28$ Å, $b = 63.33$ Å, $c = 55.07$ Å, $\alpha = \gamma = 90°$, and $\beta = 110.08°$ and contained two molecules per asymmetric unit. Further crystallographic refinement was carried out with Refmac, Phenix, and CNS and alternated with manual rebuilding using the interactive graphics program Coot. The final models of the two PILRα–GlcNAc-type glycopeptide and –deoxy-GlcNAc-type glycopeptide complexes were refined to an $R_{free}$ factor of 26.9% and an $R$ factor of 21.5% in PILRα–GlcNAc-type glycopeptide and an $R_{free}$ factor of 26.2% and an $R$ factor of 21.6% in PILRα–deoxy-GlcNAc-type glycopeptide. Detailed crystallographic statistics are shown in Table 2. The coordinates for the refined PILRα–GlcNAc and –deoxy-type glycopeptide complex structures have been deposited in the Protein Data Bank (codes 5XOF and 5XO2, respectively).

*Author contributions*—A. F. and K. M. designed the study and wrote the paper. A. F., T. Y., and T. O. performed the X-ray study. A. F., T. Y., M. I., J. S., N. M., F. O., T. S., T. N., and Ki. K. performed the ITC study. Ko. K., N. H., H. N., S. M., M. A., and S. H. synthesized glycopeptides. A. F., A. H., and K. M. discussed the results. All authors analyzed the results and approved the final version of the manuscript.

*Acknowledgments—We thank Dr. S. Kollnberger and Dr. T. A. Bowden for discussion. We also thank the beamline staff at SPring-8 for technical help during data collection.*

### References

1. Shiratori, I., Ogasawara, K., Saito, T., Lanier, L. L., and Arase, H. (2004) Activation of natural killer cells and dendritic cells upon recognition of a novel CD99-like ligand by paired immunoglobulin-like type 2 receptor. *J. Exp. Med.* **199,** 525–533
2. Fournier, N., Chalus, L., Durand, I., Garcia, E., Pin, J. J., Churakova, T., Patel, S., Zlot, C., Gorman, D., Zurawski, S., Abrams, J., Bates, E. E., and Garrone, P. (2000) FDF03, a novel inhibitory receptor of the immunoglobulin superfamily, is expressed by human dendritic and myeloid cells. *J. Immunol.* **165,** 1197–1209
3. Kuroki, K., Furukawa, A., and Maenaka, K. (2012) Molecular recognition of paired receptors in the immune system. *Front. Microbiol.* **3,** 429
4. Wang, J., Shiratori, I., Satoh, T., Lanier, L. L., and Arase, H. (2008) An essential role of sialylated O-linked sugar chains in the recognition of mouse CD99 by paired Ig-like type 2 receptor (PILR). *J. Immunol.* **180,** 1686–1693
5. Kogure, A., Shiratori, I., Wang, J., Lanier, L. L., and Arase, H. (2011) PANP is a novel O-glycosylated PILRα ligand expressed in neural tissues. *Biochem. Biophys. Res. Commun.* **405,** 428–433
6. Sun, Y., Senger, K., Baginski, T. K., Mazloom, A., Chinn, Y., Pantua, H., Hamidzadeh, K., Ramani, S. R., Luis, E., Tom, I., Sebrell, A., Quinones, G., Ma, Y., Mukhyala, K., Sai, T., *et al.* (2012) Evolutionarily conserved paired immunoglobulin-like receptor α (PILRα) domain mediates its interaction with diverse sialylated ligands. *J. Biol. Chem.* **287,** 15837–15850
7. Wang, J., Shiratori, I., Uehori, J., Ikawa, M., and Arase, H. (2013) Neutrophil infiltration during inflammation is regulated by PILRα via modulation of integrin activation. *Nat. Immunol.* **14,** 34–40
8. Satoh, T., Arii, J., Suenaga, T., Wang, J., Kogure, A., Uehori, J., Arase, N., Shiratori, I., Tanaka, S., Kawaguchi, Y., Spear, P. G., Lanier, L. L., and Arase, H. (2008) PILRα is a herpes simplex virus-1 entry coreceptor that associates with glycoprotein B. *Cell* **132,** 935–944
9. Kuroki, K., Wang, J., Ose, T., Yamaguchi, M., Tabata, S., Maita, N., Nakamura, S., Kajikawa, M., Kogure, A., Satoh, T., Arase, H., and Maenaka, K. (2014) Structural basis for simultaneous recognition of an O-glycan and its attached peptide of mucin family by immune receptor PILRα. *Proc. Natl. Acad. Sci. U.S.A.* **111,** 8877–8882
10. Radhakrishnan, P., Dabelsteen, S., Madsen, F. B., Francavilla, C., Kopp, K. L., Steentoft, C., Vakhrushev, S. Y., Olsen, J. V., Hansen, L., Bennett, E. P., Woetmann, A., Yin, G., Chen, L., Song, H., Bak, M., *et al.* (2014) Immature truncated O-glycophenotype of cancer directly induces oncogenic features. *Proc. Natl. Acad. Sci. U.S.A.* **111,** E4066–E4075

11. Chen, S., Rentero Rebollo, I., Buth, S. A., Morales-Sanfrutos, J., Touati, J., Leiman, P. G., and Heinis, C. (2013) Bicyclic peptide ligands pulled out of cysteine-rich peptide libraries. *J. Am. Chem. Soc.* **135,** 6562–6569
12. Zhao, B., Xu, P., Jiang, L., Paaske, B., Kromann-Hansen, T., Jensen, J. K., Sørensen, H. P., Liu, Z., Nielsen, J. T., Christensen, A., Hosseini, M., Sørensen, K. K., Nielsen, N. C., Jensen, K. J., Huang, M., *et al.* (2014) A cyclic peptidic serine protease inhibitor: increasing affinity by increasing peptide flexibility. *PLoS One* **9,** e115872
13. Lu, Q., Lu, G., Qi, J., Wang, H., Xuan, Y., Wang, Q., Li, Y., Zhang, Y., Zheng, C., Fan, Z., Yan, J., and Gao, G. F. (2014) PILRα and PILRβ have a siglec fold and provide the basis of binding to sialic acid. *Proc. Natl. Acad. Sci. U.S.A.* **111,** 8221–8226
14. Halim, A., Rüetschi, U., Larson, G., and Nilsson, J. (2013) LC-MS/MS characterization of O-glycosylation sites and glycan structures of human cerebrospinal fluid glycoproteins. *J. Proteome Res.* **12,** 573–584
15. Nagae, M., Morita-Matsumoto, K., Kato, M., Kaneko, M. K., Kato, Y., and Yamaguchi, Y. (2014) A platform of C-type lectin-like receptor CLEC-2 for binding O-glycosylated podoplanin and nonglycosylated rhodocytin. *Structure* **22,** 1711–1721
16. Kakita, K. (2016) *Synthesis of Sialyl TN-Antigen Containing Glycopeptides as Inhibitors of Herpes Simplex Virus Type 1 Infection Based on Glycosyl Donors Carrying Phosphorus-Containing Leaving Groups*. Doctoral thesis, Hokkaido University
17. Tabata, S., Kuroki, K., Wang, J., Kajikawa, M., Shiratori, I., Kohda, D., Arase, H., and Maenaka, K. (2008) Biophysical characterization of *O*-glycosylated CD99 recognition by paired Ig-like type 2 receptors. *J. Biol. Chem.* **283,** 8893–8901
18. Shiroishi, M., Tsumoto, K., Amano, K., Shirakihara, Y., Colonna, M., Braud, V. M., Allan, D. S., Makadzange, A., Rowland-Jones, S., Willcox, B., Jones, E. Y., van der Merwe, P. A., Kumagai, I., and Maenaka, K. (2003) Human inhibitory receptors Ig-like transcript 2 (ILT2) and ILT4 compete with CD8 for MHC class I binding and bind preferentially to HLA-G. *Proc. Natl. Acad. Sci. U.S.A.* **100,** 8856–8861
19. Zeraik, A. E., Pereira, H. M., Santos, Y. V., Brandão-Neto, J., Spoerner, M., Santos, M. S., Colnago, L. A., Garratt, R. C., Araújo, A. P., and DeMarco, R. (2014) Crystal structure of a *Schistosoma mansoni* septin reveals the phenomenon of strand slippage in septins dependent on the nature of the bound nucleotide. *J. Biol. Chem.* **289,** 7799–7811
20. Tellinghuisen, J. (2008) Isothermal titration calorimetry at very low c. *Anal. Biochem.* **373,** 395–397
21. McCoy, A. J., Grosse-Kunstleve, R. W., Adams, P. D., Winn, M. D., Storoni, L. C., and Read, R. J. (2007) Phaser crystallographic software. *J. Appl. Crystallogr.* **40,** 658–674

# Structural and thermodynamic analyses reveal critical features of glycopeptide recognition by the human PILR α immune cell receptor

Atsushi Furukawa, Kosuke Kakita, Tomoki Yamada, Mikihiro Ishizuka, Jiro Sakamoto, Nanao Hatori, Naoyoshi Maeda, Fumina Ohsaka, Takashi Saitoh, Takao Nomura, Kimiko Kuroki, Hisanori Nambu, Hisashi Arase, Shigeki Matsunaga, Masahiro Anada, Toyoyuki Ose, Shunichi Hashimoto and Katsumi Maenaka

*J. Biol. Chem. 2017, 292:21128-21136.*
*doi: 10.1074/jbc.M117.799239 originally published online October 18, 2017*

---